

AD 684462

Technical Note N-780

NUCLEAR BLAST VULNERABILITY OF SHELTER ELECTRICAL GENERATING
EQUIPMENT - DIESEL ENGINE OVERPRESSURE TOLERANCE

by

Jerar Andon

November 1965

DDC
RECEIVED
MAR 28 1969
RECEIVED
B

CLEARED FOR UNLIMITED DISTRIBUTION

Best Available Copy

U. S. NAVAL CIVIL ENGINEERING LABORATORY
Port Hueneme, California

Reproduced by the
CLEARINGHOUSE
for Federal Scientific & Technical
Information Springfield Va. 22151

This document has been approved
for public release and sale; its
distribution is unlimited

NUCLEAR BLAST VULNERABILITY OF SHELTER ELECTRICAL GENERATING
EQUIPMENT - DIESEL ENGINE OVERPRESSURE TOLERANCE

Y-F011-05-02-306

by

Jerar Andon

ABSTRACT

Nuclear blast tolerance of internal parts of an operating diesel engine was tested by exposing the exhaust system, and simultaneously the intake and exhaust system to simulated overpressure air. Peak overpressures as high as 100 psi were applied. When the engine exhaust was subjected to overpressure, the engine speed was momentarily but noticeably reduced and the combustion chamber peak pressure was slightly increased. With the intake and exhaust system exposure to overpressures, the engine speed was only slightly affected and the peak combustion chamber pressure was greatly increased. This pressure reached 4400 psi at 100 psi overpressure, thus increasing the internal load to over four times that of normal engine operation. The diesel engine under test withstood repeated overpressure applications of 100 psi without any failures.

To complete the evaluation of blast vulnerability of diesel-driven generator sets, external parts tolerance tests will be necessary.

~~Each transmission element outside the~~
~~prior, Andon, 1952, U.S. Naval Engineering Laboratory~~

INTRODUCTION

Nuclear blast tests¹ of electrical generating equipment located in pits, and shock tube tests² of model size pits have indicated that the engine-generator set can be comparatively easily protected from blast dynamic pressure but protection against blast overpressure is more difficult. Consequently, a comprehensive research program was formulated by this Laboratory to determine the tolerance of an operating diesel engine-generator to blast overpressure. The first task in the program, covered by this report, was restricted to the internal parts tolerance.

Two series of tests were carried out, representing different engine locations with regard to nuclear blast overpressure exposure. The first series simulated an engine-generator set located in a protective shelter with its exhaust system exposed to atmosphere and its intake system protected by shelter blast closure valves. The second series simulated an engine-generator set located in a protected pit with both intake and exhaust systems of the engine exposed to blast overpressure.

The exhaust exposure to overpressure was not considered as severe as the case where both intake and exhaust were exposed to the overpressure. The analysis of engine operation indicated that with its exhaust system exposed to overpressure, the engine would slow down due to increased back pressure, or even stop if the pressure in the exhaust was great enough for a long enough period to overcome engine and generator rotating inertia and engine exhaust blow-down pressure. However, with the intake manifold exposed to overpressure, the engine would be charged with high pressure air, whose pressure will be further increased during the engine compression stroke. The high compression peak pressure could conceivably cause failure of internal parts of the engine. Before the tests, there was considerable doubt concerning the engine internal parts successfully operating under this type of loading.

NUCLEAR BLAST OVERPRESSURE CHARACTERISTICS

The ideal peak overpressure values and the duration of the positive phase of the overpressure for a one MT nuclear explosion are listed in Table I³.

TABLE I

One MT Nuclear Burst at Optimum Burst Height

Peak overpressures (psi)	Duration of positive phase (sec)	Distance from ground zero (mile)
100	1.0	.72
70	1.2	.86
50	1.5	1.04
30	1.8	1.40
20	2.1	1.77
10	2.7	2.70
5	3.4	4.30

These ideal overpressure-time diagrams are shown in Figure 1. The overpressure suddenly builds up to a peak pressure and then decays exponentially down to zero for the positive phase of the overpressure. The positive phase duration is longer for the lower overpressures. The negative phase of the overpressure, not shown in Figure 1, produces a low amplitude negative pressure. Since the positive phase is the most detrimental to an operating engine, the effect of only this part of the overpressure has been analyzed.

Figure 2 shows the number of engine cycles that occur during the passing of a 50 psi overpressure phenomenon. Approximately 22 engine cycles are shown on this curve. It is apparent that the engine cycle is an event of very short duration when compared to the positive phase of overpressure. Hence, it is proper to approximate the overpressure as constant during a cycle, but different for each subsequent engine cycle.

TEST EQUIPMENT

Air Blast Equipment

An air blast device was developed to supply simulated overpressure air to the intake and exhaust systems of the engine. Figure 3 shows the basic components of this device which are:

1. Supply tank
2. Diaphragm
3. Nozzle
4. Connection to the engine air flow system

The supply tank can be pressurized to any pressure up to 100 psig using a diaphragm to contain the pressure in the tank. Since the tank pressure is close to the bursting pressure of the diaphragm, a small puncture of the diaphragm will cause the diaphragm to suddenly rupture. The air flows through a nozzle selected with an entrance/exit area ratio so that the pressure in the tank will decay approximately in the same manner as the ideal overpressures. Figure 4 shows actual pressure-time diagrams, measured at the entrance of the nozzle, compared with the ideal calculated overpressure-time data. It will be noted that the actual measured pressure goes to the peak value in approximately 5 milliseconds and drops off in approximately the same manner as the ideal overpressure curve. The nozzle area ratios used, which give approximately the desired pressure decay for the various overpressures, are shown in Table II.

TABLE II

Nozzle Dimensions

Peak Overpressure psi	Entrance Area sq. in.	Exit Area sq. in.	Ratio Entrance/Exit
100	56.6	23.8	2.28
50	56.6	12.6	4.48
30	56.6	9.8	5.78
20	56.6	4.5	12.57
10	56.6	2.4	23.6

The nozzle entrance area was fixed by the dimensions of existing tank and diaphragm holder. The exit area was determined by using nozzle flow calculations. For most nozzles the flow was initially critical. Once the pressure ratio between nozzle entrance and exit dropped below the critical, the flow changed to normal flow. To approximate these conditions, short time increments of constant air pressures in the tank were used to calculate the flow in both regions.

Figure 5 shows the actual test arrangement for the combined intake and exhaust overpressure tests. For the exhaust overpressure tests, the air intake pipe was removed and the normal air intake cleaner was used. Figure 6 is a closeup view of the nozzle and also shows the engine air flow system connections. The exhaust system has a flapper valve arrangement which would swing up and close when the pressure in the nozzle was higher than atmospheric. This flapper valve would keep the engine exhaust gas from contaminating the intake air before and after overpressure applications.

Pressure Measuring Instrumentation

Pressure measuring equipment consisted of quartz pressure transducers, electrostatic charge amplifiers, and power amplifiers. Each pressure channel was fed into a high frequency galvanometer and recorded by an oscillograph. The pressure transducers were fitted with adaptors and installed in the engine combustion chamber, engine intake manifold, engine exhaust manifold, and various other positions on the air blast equipment. Figures 7 and 8 show the locations of the pressure transducers in the engine combustion chamber, intake and exhaust systems. From pressure measurements at the points indicated, the effect of the overpressure in the intake and exhaust systems was ascertained.

The combustion chamber pressure measurement represents the loading on the engine parts. The data thus obtained can be applied with reasonable confidence not only to the particular test engine, but can also be extended to other engines of similar design if the load carrying characteristics of the engine parts are known.

THE DIESEL ENGINE CYCLE

Prior to discussing the overpressure effects on the engine, the following review of the normal diesel engine cycle is necessary. The diesel cycle is normally represented by a pressure-volume (PV) diagram, and Figure 9 shows an idealized diesel cycle diagram. The solid lines represent the engine full load operation, and the broken lines and bottom solid lines represent the engine operation at approximately half load.

The diesel cycle consists of the following processes:

- 0 - 1 Constant pressure intake
- 1 - 2 Polytropic compression
- 2 - 2' Constant volume combustion
- 2' - 3 Constant pressure combustion
- 3 - 4 Polytropic expansion
- 4 - 1 Constant volume exhaust blowdown
- 1 - 0 Constant pressure exhaust

The pressure values in the typical diesel engine are listed below:

	<u>Full Load</u>		<u>Half Load</u>
P_1	= 14.2 psia	F_1	= 14.2 psia
P_2	= 700 psia	P_2	= 700 psia
P_2, P_3	= 1000 psia	P_2, P_3	= 850 psia
P_4	= 70 psia	P_4	= 30 psia

The pressure and temperature calculations for each process making up the complete engine cycle shown on the PV diagram are described by Taylor and Taylor⁴. Generally the peak compressive pressure P_2 can be easily calculated by the expression

$$P_2 = P_1 \left(\frac{V_1}{V_2} \right)^n = P_1 r^n$$

where

P_1 = initial intake pressure, psia

P_2 = peak compressive pressure, psia

V_1 = displacement volume plus combustion chamber volume, cu. in.

V_2 = combustion chamber volume, cu in.

r = compression ratio = $\frac{V_1}{V_2}$

n = polytropic exponent for compression process

The irreversibility of the compression process due to some heat loss and air leakage through the valves and piston rings can be accounted for by using a lower value for the exponent n . The exponent used in this study to obtain 700 psia for peak compressive pressure with an initial intake pressure of 14.2 psia is 1.30. Further increase in pressure due to combustion depends on the fuel injection timing, fuel injection duration and fuel spray form. The peak firing pressure is very difficult to calculate without detailed knowledge of the above mentioned fuel injection parameters, however, in an ordinary diesel engine the peak pressure is usually limited to 1000 psia.

A 32 hp, 1800 rpm, Waukesha diesel engine driving a 10 kw generator was used for the test. The engine specifications are given in Appendix A. The engine was operating at half-load and its pressure-time diagram is shown in Figure 10. This pressure-time diagram can be converted to a PV diagram similar to the half-load cycle represented in Figure 9.

The engine cycle processes are shown in Figure 11 as time events of one engine cycle. The intake and exhaust events are indicated as well as the pressure-time diagrams for each of the four cylinders.

EXHAUST SYSTEM OVERPRESSURE TOLERANCE

Simulated overpressure conditions were applied to the exhaust system to determine the effects on engine operation. Peak overpressures of 10, 20, 30, 50, 70 and 100 psi were applied to the exhaust system while the engine was running at 1800 rpm at half-load conditions. Very little change in engine combustion chamber peak pressure or engine speed was noted during the 10, 20 and 30 psi overpressure applications. Figure 12 shows the test record for the 100 psi peak overpressure application to the exhaust system. Pressure-time diagrams for the exhaust system, intake system and combustion chamber are shown. A large oscillation of the exhaust system pressure is apparent when the exhaust system pressure in Figure 12 is compared to the applied overpressure-time diagram in Figure 4. In all of these overpressure applications, in both intake and exhaust systems, there is an overshoot of pressure in the beginning and an oscillation of pressure about the applied overpressure.

Variations of combustion chamber peak pressure and engine speed due to overpressure application are shown in Figure 13. At 50, 70 and 100 psi, the combustion chamber peak pressure increases after overpressure application and the engine momentarily slows down. The drop in speed gets larger as the applied overpressure is higher. It is apparent that the engine would stop at some overpressure application higher than 100 psi. The combustion chamber peak pressure increases because more fuel is injected into the chamber when the engine slows down. Increased exhaust system back pressure caused by the overpressure has the same effect on the engine as increased load on the engine. The governor, sensing a speed drop, will compensate for it by increasing the amount of fuel injected. With the increased amount of fuel, some of the engine cycles operated at full load and produced combustion pressures as high as 1050 psi.

No apparent failures were noted after these overpressure applications, and the engine running characteristics remained unchanged. Except for speed reduction, no unusual engine behavior was noted during the overpressure applications.

INTAKE AND EXHAUST SYSTEM TOLERANCE

Simulated overpressure conditions were also applied to the intake and exhaust system simultaneously. Overpressures of 10, 20, 30, 50, 70 and 100 psi were applied to the combined intake and exhaust systems when engine was operating at half load and 1800 rpm. The effect of 10 psi overpressure application was insignificant. With higher overpressure applications, the combustion chamber pressure substantially increased as expected. Figure 14 shows oscillograms of 50, 70 and 100 psi applications which are pressure-time records of the intake system, exhaust

system, and the combustion chamber. Two normal engine cycles are shown before the overpressure application. The combustion chamber pressure increase is readily seen after the overpressure application. The engine speed variation was slight for all intake-exhaust overpressure applications with the maximum reduction being approximately 10 per cent at 100 psi overpressure.

The primary measurement for this test is the combustion chamber peak pressure, since this measurement determines the internal load on the principal parts of the engine. The combustion chamber walls, intake and exhaust valves, piston and piston rings, and cylinder head gasket, are directly affected by the increased pressure in the combustion chamber. The piston, piston wrist pin, connecting rod and bearings, crankshaft and bearings, and the crankcase, are affected indirectly by increased loads due to higher combustion chamber pressure. The internal tolerance of the engine to overpressure depends on how well these parts withstand the momentary overloading due to overpressure application. These parts are designed for long fatigue life, and the diesel engine is usually designed for higher fatigue life than other types of internal combustion engines. Higher fatigue life for a loaded part generally means higher momentary load capacity. The experiment confirmed this generalization as no failures of internal parts occurred during the tests.

The peak combustion chamber pressure for a number of engine cycles was measured and the results are plotted in Figure 15 for simultaneous 20, 30, 50, 70 and 100 psi overpressure applications to engine intake and exhaust. The data shows the peak compressive pressure and the peak firing pressure due to combustion for 10 cycles before overpressure application and 30 cycles after. It is apparent from this data that the compressive peak pressure varies directly in proportion to the magnitude of overpressure. To illustrate this, the peak combustion chamber pressures for the 30, 50, 70 and 100 psi overpressure tests are plotted with respect to overpressure occurring during each cycle in Figure 16. A straight line fits best most of the data indicating this to be a direct proportionality.

The maximum compressive pressure in the combustion chamber during the tests was 4400 psi for 100 psi overpressure. Table III lists the maximum combustion chamber pressure for the various overpressure applications.

TABLE III

Maximum Pressures (psi)

<u>Overpressure</u>	<u>Combustion Chamber</u>	
	<u>Compression</u>	<u>Firing</u>
20	1600	1860
30	2000	2250
50	2850	3700
70	3800	4100
100	4400	Not Firing

Using the relationship discussed earlier,

$$P_2 = P_1 (r)^n$$

to calculate the peak compressive pressure P_2 , using P_1 as the average pressure of the intake system, and r as the compression ratio, one must vary the exponent n from 1.30 for compression from normal atmospheric pressure to 1.24 from 100 psi overpressure. This decrease represents the increased leakage through the piston rings and valves, and the higher rate of heat transfer during compression.

For normal combustion, the pressure increase due to firing varies from cycle to cycle with the maximum increase of 250 psi and an average of 125 psi increase over the pressure due to compression. During the overpressure application the maximum firing pressure increase over that of peak compression pressure was 500 psi, and the average increase approximately 200 psi. For the extremely high compression cycles no additional pressure increase, due to combustion of fuel, was noted. Evidently the fuel was not injected properly in the combustion chamber for these high compressive pressures, which resulted in engine misfiring. Although the firing of the engine, immediately after each high overpressure application, was very rough, the engine would still carry the load. A few minutes of running after the overpressure had passed, the engine invariably settled down to normal smooth operation.

The 100 psi overpressure was applied to the engine three times with no failures occurring. The engine was disassembled, and the principal parts were inspected. No damage or unusual wear was noted during this inspection.

FINDINGS

1. Table IV summarizes the results of overpressure application to the test engine exhaust system and Table V to the test engine exhaust and intake systems simultaneously.

TABLE IV. Exhaust Overpressure Tests

<u>Date</u>	<u>Run No.</u>	<u>Peak Overpressure psi</u>	<u>Remarks</u> <u>Combustion Chamber Pressure</u> <u>Minimum Engine Speed</u>
17 May 65	1	10	No change - 825 psi chamber pressure 1800 rpm speed
	2	20	900 psi max chamber pressure 1800 rpm speed
	3	30	870 psi max chamber pressure 1800 rpm speed
	4	50	930 psi max chamber pressure 1770 rpm speed
	5	70	1050 psi max chamber pressure 1500 rpm speed
8 Jun 65	1	100	1000 psi max chamber pressure 1270 rpm speed

TABLE V. Intake and Exhaust Overpressure Tests

<u>Date</u>	<u>Run No.</u>	<u>Peak Overpressure psi</u>	<u>Remarks</u>
8 Jun 65	2	10	1250 ps. max chamber pressure
	3	20	1700 psi max chamber pressure
9 Jun 65	1	20	1860 psi max chamber pressure
	2	30	2250 psi max chamber pressure
	3	50	No max pressure measurement available
	4	70	No max pressure measurement available
	5	100	No max pressure measurement available
14 Jun 65	1	50	3200 psi max chamber pressure
	2	70	4100 psi max chamber pressure
	3	100	4400* psi max chamber pressure
	4	100	4400* psi max chamber pressure

*Engine failed to fire on this cycle.

2. The high overpressure application to the exhaust system resulted in a momentary reduction of engine speed and a slight increase of the peak combustion chamber pressure.

3. The simultaneous application of overpressure to the intake and exhaust systems affect engine speed but very little, however, the combustion chamber peak pressure was greatly increased and reached 4400 psi for the 100 psi overpressure application. The engine was misfiring at high combustion chamber pressures which indicates that the high pressures were the result of compression process rather than of the combustion of fuel.

4. The engine ran successfully during the entire test program. No failures of internal parts were noted after the tests.

CONCLUSIONS

1. The Waukesha 180 DLC diesel engine can tolerate internally blast overpressures up to 100 psi applied simultaneously to the engine exhaust and intake systems.

2. To predict the tolerance of another engine, using the results of these tests, would require a comparison of the internal parts of the tested engine and the other engine. The load carrying capacity of the other engine will have to be at least as high as the engine used for these tests.

RECOMMENDATIONS

To complete the evaluation of blast vulnerability of diesel-driven generator sets, external parts tolerance tests will be necessary. It is recommended that these tests be conducted as soon as possible, using the same engine-generator set and test equipment that were used for the internal parts tolerance tests.

REFERENCES

1. Defense Atomic Support Agency, WT-1422, "Operation Plumbbob, Evaluation of Buried Corrugated-Steel Arch Structures and Associated Components," by G. H. Albright, et al., Washington, D. C., 28 February 1961.
2. U. S. Naval Civil Engineering Laboratory. Technical Report R-274, "Model Studies of Large Vented Openings - Phase I," by Donald S. Teague, Jr., Port Hueneme, California, 5 March 1964.
3. U. S. Department of Defense. "The Effects of Nuclear Weapons," United States Atomic Energy Commission, Washington, D. C., April 1962.
4. Taylor, C. F., and Taylor, E. S., "The Internal Combustion Engine," International Textbook Co., 1961, pp 57-59.
5. Shapiro, A. H., "The Dynamics and Thermodynamics of Compressible Fluid Flow," The Ronald Press, 1953, pp 159-186.

APPENDIX A

PRINCIPAL ENGINE SPECIFICATIONS

WAUKESHA 180 DLC ENGINE

Type - 4-stroke diesel with precombustion chamber

Bore and stroke - 3-1/2 in. x 3-3/4 in.

Number of cylinders and arrangement - 4-in-line

Displacement - 144 cu. in.

Compression Ratio - 19 to 1

Valve arrangement - overhead

Number of main bearings - 3

Firing order - 1-2-4-3

Weight - 750 lbs.

APPENDIX B

ENGINE SYSTEM AND FLUID DYNAMICS

The engine intake and exhaust systems are illustrated in Figure B-1. Either the intake or exhaust system may be represented by a simple long constant area duct with a nozzle on the inlet end to represent the air cleaner or exhaust muffler. The simple system may now be analyzed by one-dimensional compressible fluid flow dynamics.

For normal engine operation the pressure drops from 14.7 psia at the inlet of the air flow duct to 14.2 psia at the end of the duct. The value of 0.5 psia pressure drop is typical of this type of engine running at the speed of 1800 rpm. The rest of the air flow data for the Waukesha engine is as follows:

$$\text{Velocity in duct, } V = 120 \text{ ft/sec}$$

$$\text{Temperature, } T = 100 \text{ F} = 560 \text{ R}$$

$$\text{Viscosity, } \nu = 1.8 \times 10^{-4} \text{ ft}^2/\text{sec}$$

Using 1.125 inches for the diameter of the duct D , the Reynolds Number may be calculated

$$Re_D = \frac{VD}{\nu} = \frac{120(1.125)}{1.8(10^{-4})12} = 6.25(10^4)$$

Since cast iron is used as the duct walls, roughness is

$$e = 0.00085 \text{ ft}$$

$$\frac{e}{D} = \frac{0.00085}{\frac{1.125}{12}} = 0.00907$$

From the Moody diagram the friction factor is

$$f = 0.036$$

The velocity of sound C , in the assumed system is

$$C = 49.02 \sqrt{560} = 49.02 \sqrt{560} = 1160 \text{ ft/sec}$$

Then, the Mach number is

$$M = \frac{V}{C} = \frac{120}{1160} = 0.103$$

If we assume isothermal flow with friction, the equivalent length of the duct can be determined. For a horizontal pipe of constant pipe section, the momentum equation is

$$\sum F_x = \dot{m} \Delta V_x$$

where $\sum F_x$ is the summation of forces in the duct length direction, \dot{m} is the mass flow rate and ΔV_x is the change in velocity.

For our system the momentum equation can be written as

$$P \frac{\pi D^2}{4} - (P+dP) \frac{\pi D^2}{4} - \tau_w \pi D dx = v \frac{\pi D^2}{4} \rho dv$$

where τ_w , the wall shear stress, may be expressed as

$$= \frac{f \rho V^2}{8}$$

and where P is the pressure, x is the distance along the duct length and ρ is the density.

Inserting this in the momentum equation and rearranging

$$\frac{dP}{\rho V^2} + f \frac{dx}{D} + 2 \frac{dv}{V} = 0$$

From perfect gas equation of state

$$\rho = P \frac{\rho_i}{P_i}$$

where the subscript i is the entrance to the duct.

From continuity

$$v \rho = v_i \rho_i$$

Then

$$v = \frac{v_i P_i}{P}$$

the differential form of this last equation is

$$\frac{dV}{V} + \frac{dP}{P} = 0 \quad \text{or} \quad \frac{dV}{V} = -\frac{dP}{P}$$

The first term of the momentum equation can now be written

$$\left(\frac{\rho V^2}{P} \right) P dP$$

Integrating the momentum equation and using $L = x_e - x_i$ as the length of duct, since e is the exit point, we obtain

$$P_i^2 - P_e^2 = \rho_e V_i^2 \left(f \frac{L}{D} - 2 \ln \frac{P_i}{P_e} \right)$$

since $V^2 = M^2 C^2 = M^2 kRT$ and $P = \rho RT$

$$P_i^2 - P_e^2 = k M_i^2 P_i^2 \left(f \frac{L}{D} - 2 \ln \frac{P_i}{P_e} \right)$$

or

$$1 - \left(\frac{P_e}{P_i} \right)^2 = k M_i^2 \left(f \frac{L}{D} - 2 \ln \frac{P_i}{P_e} \right)$$

If $P_i = 14.7$ psia and $P_e = 14.2$ psia

$$\frac{P_e}{P_i} = \frac{14.2}{14.7} = 0.966 \quad \text{and}$$

$$\frac{P_i}{P_e} = \frac{14.7}{14.2} = 1.035$$

$$1 - (0.966)^2 = 1.4(0.103)^2 \left[(0.036) \frac{L}{1.125} - 2 \ln (1.035) \right]$$

$$L = 11.9 \text{ ft or } 143 \text{ in.}$$

The actual intake system of the engine is approximately 50 inches long. There are three 90-degree bends in the system. Using the general practice of adding 30 inches length for each bend, the equivalent length would be 140 inches, which makes the above calculations and assumptions reasonable.

When the assumed system is first exposed to overpressure, critical flow will take place. With

$$\frac{fL_{\max}}{D} = \frac{(0.036)(143)}{1.125} = 4.57$$

critical flow calculations listed in Shapiro⁵, Table B4, "Frictional Adiabatic, Constant Area Flow" (Fanno Line) gives

$$M_1 = 0.32$$

$$M_e = 1.00$$

$$\frac{P_1}{P^*} = 3.44$$

where subscript 1 is duct entrance, subscript e is exit and * is the critical point.

Then from Table B2, "Isentropic Flow", for $M_1 = 0.32$

$$\frac{P_1}{P_o} = 0.932$$

where subscript o is the surrounding.

or

$$P_1 = 0.932P_o$$

since

$$P^* = \frac{P_1}{3.44} = \frac{0.932P_o}{3.44} = 0.271P_o$$

Once the pressure P_2 rises above $0.271P_0$, the flow is not critical and there will be normal isentropic flow without shock. Both normal isentropic flow and flow with shock were calculated for various overpressures P_0 and shown in Figure B-2.

The assumed system will have Fanno flow (with friction) without shock occurring in the duct during most of the time of overpressure except for the first instant the overpressure occurs. This exception is illustrated by Case I in Figure B2. During the first overpressure exposure, the exit pressure P_e is lower than the critical pressure; therefore, shock would occur at the exit end of the duct. The exit pressure increases rapidly to above critical pressure during the first engine cycle, thereby giving normal flow illustrated by Cases II through VII. The pressure in the engine cylinder would only be slightly lower than the outside overpressure. Critical flow conditions would not occur long enough to cause any appreciable decrease in air flow.

Figure B3 shows the actual pressure-time diagrams measured in the entrance to the nozzle and engine intake system. These pressure records show very little decrease in the pressure from nozzle to intake system. In fact, there is an overshoot of pressure which oscillates about the applied overpressure in the intake system. This type of oscillation is generally expected with such a sudden overpressure application. The frequency of this oscillation is determined by the system dimensions which, in turn, determines the mass of the system. The shock wave occurring at the beginning of the intake system pressure-time diagram substantiates the above remarks concerning critical flow.

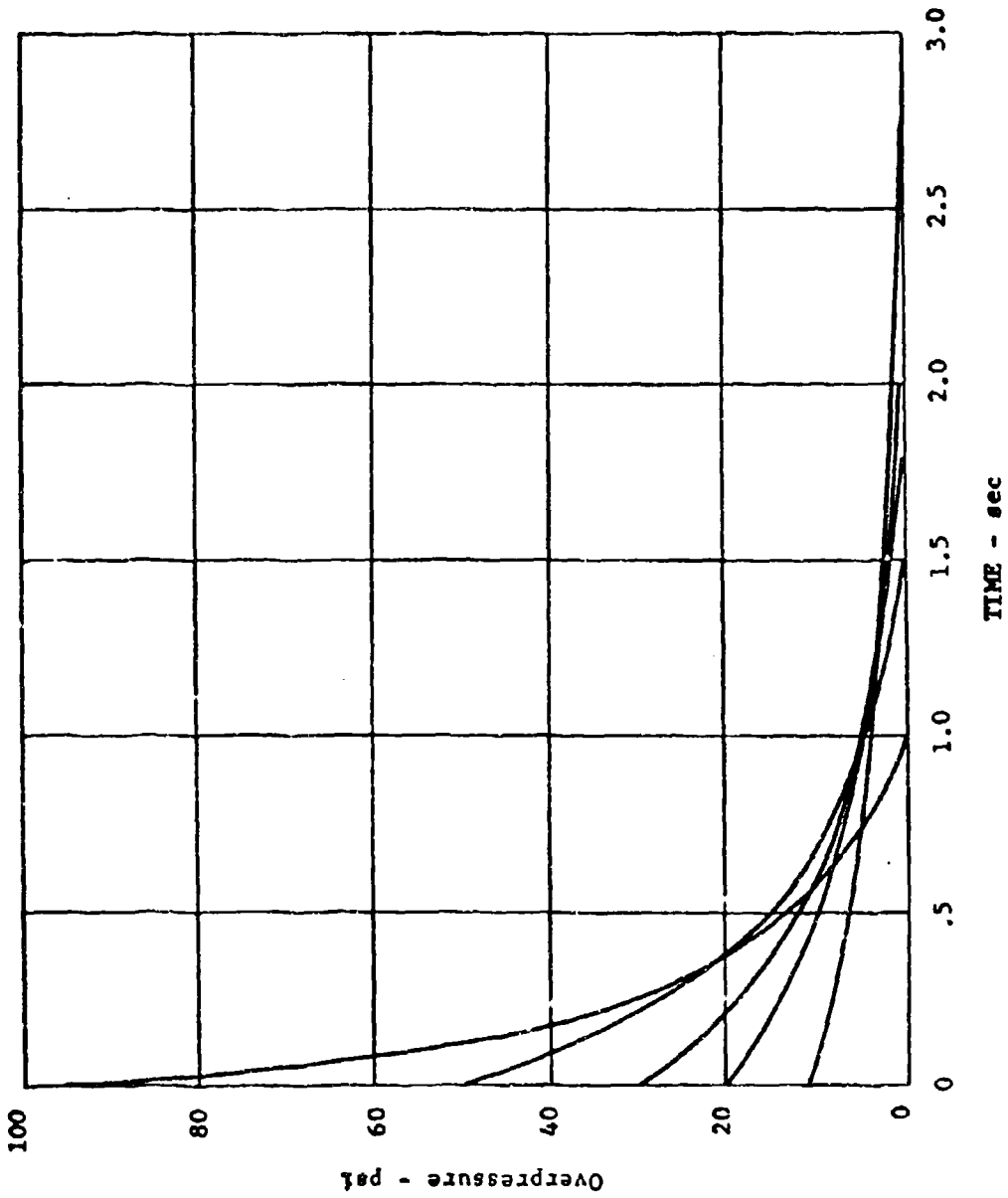


Figure 1. Ideal overpressure-time diagrams for various peak overpressures.

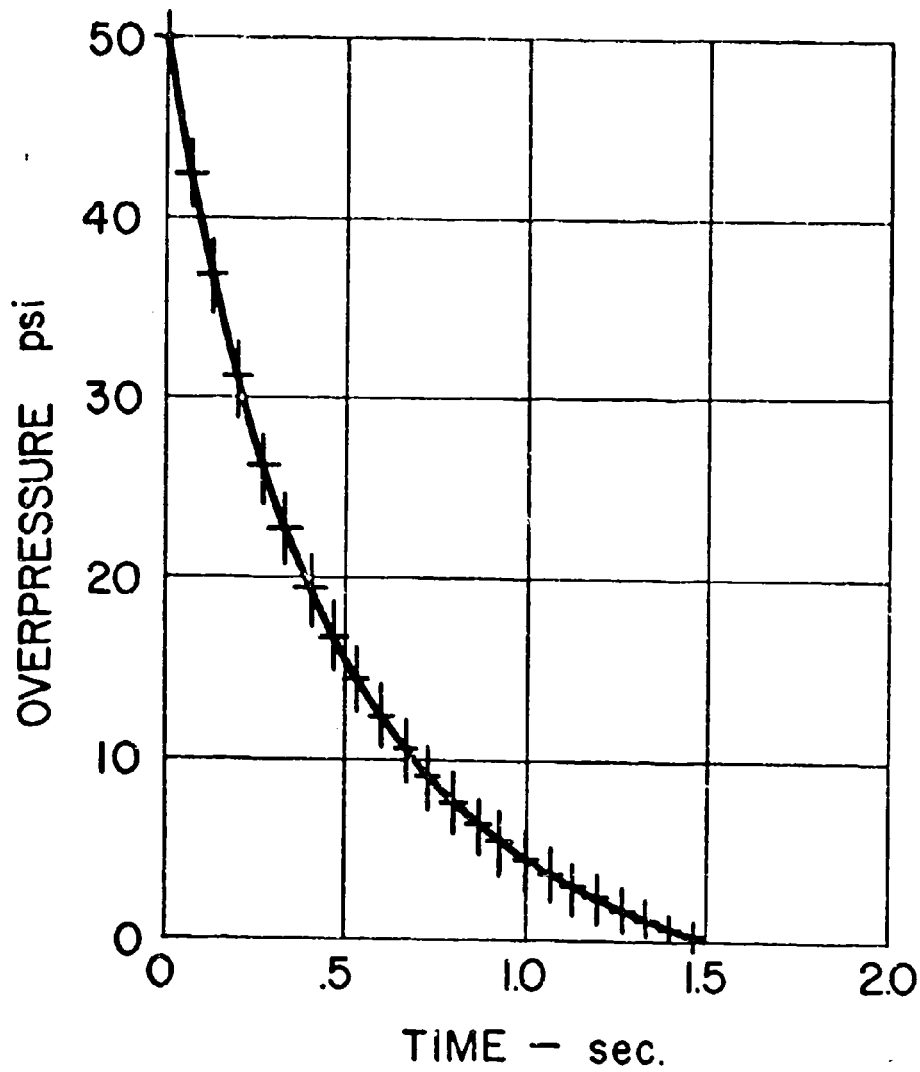


Figure 2. The 50 psi peak overpressure-time curve with timing marks (vertical lines) showing engine cycles that occur when engine is operating at 1800 rpm speed.

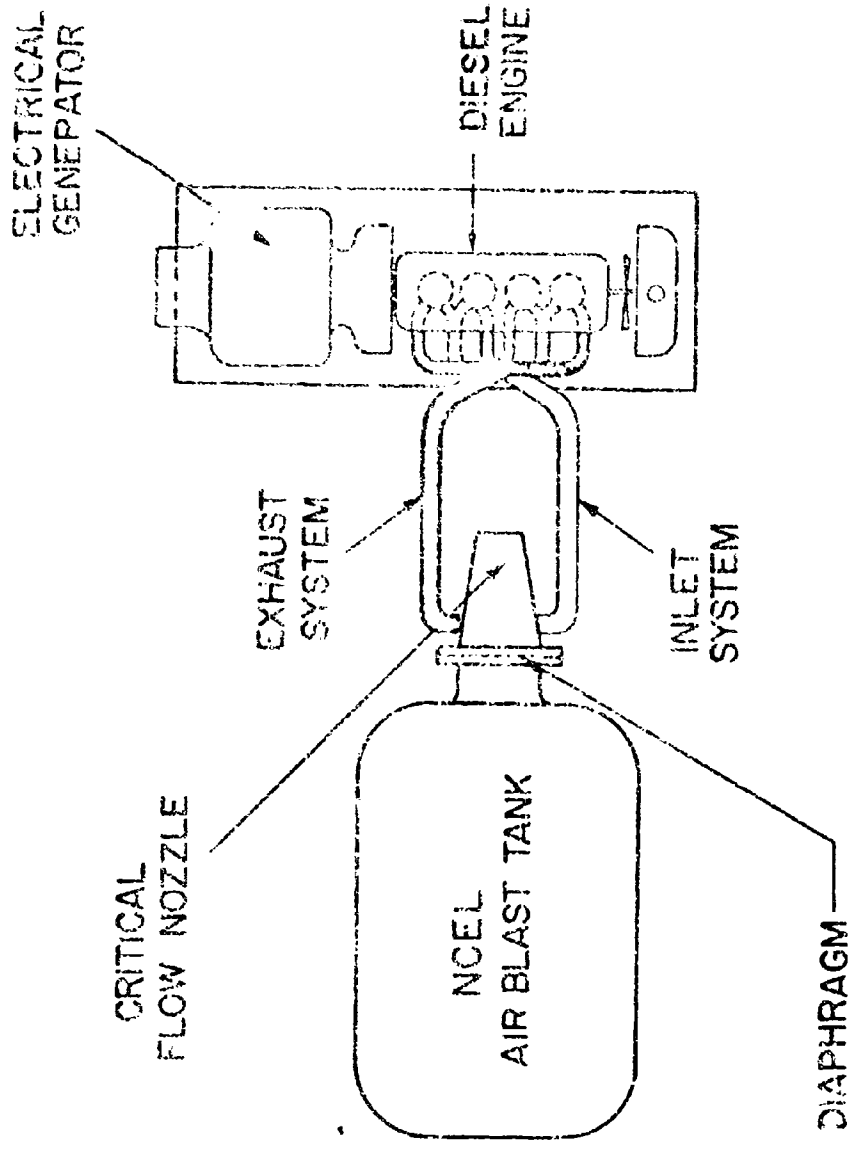


Figure 3. Basic components of the overpressure test arrangement.

○ Calculated Data for Ideal
Overpressure Curve

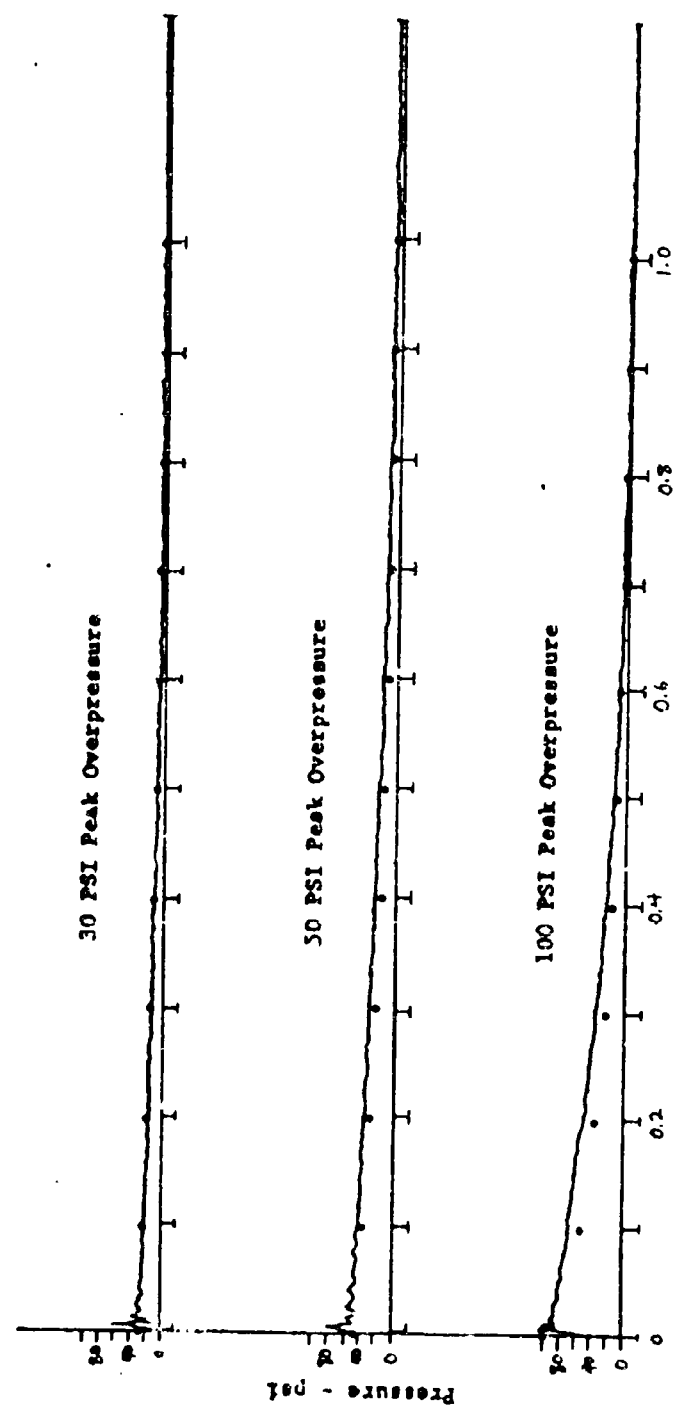


Figure 4. Overpressure-time diagrams compared with calculated ideal overpressure data.

NOT REPRODUCIBLE

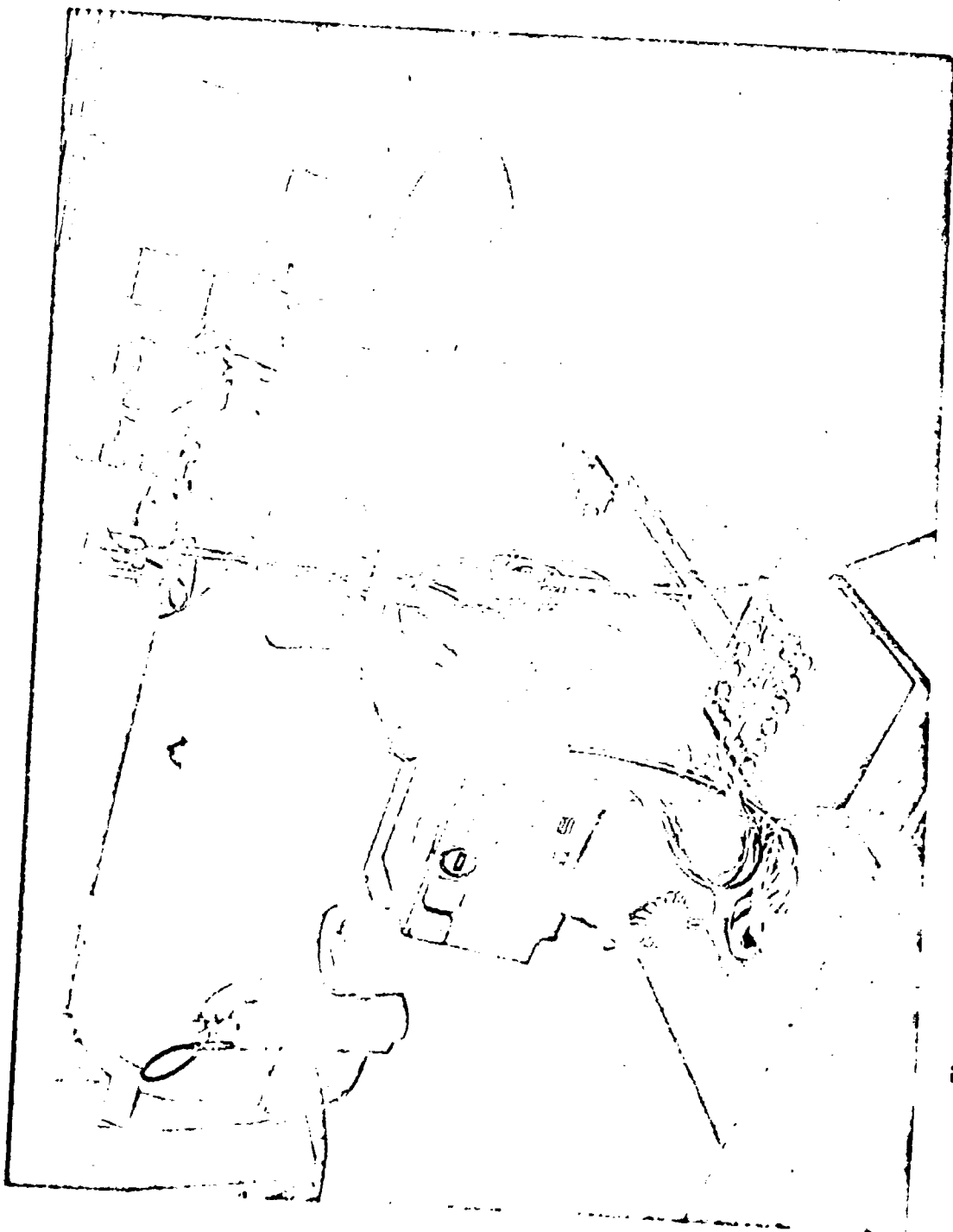


Figure 5. Test arrangement showing air blast equipment and diesel engine-generator.

NOT REPRODUCIBLE

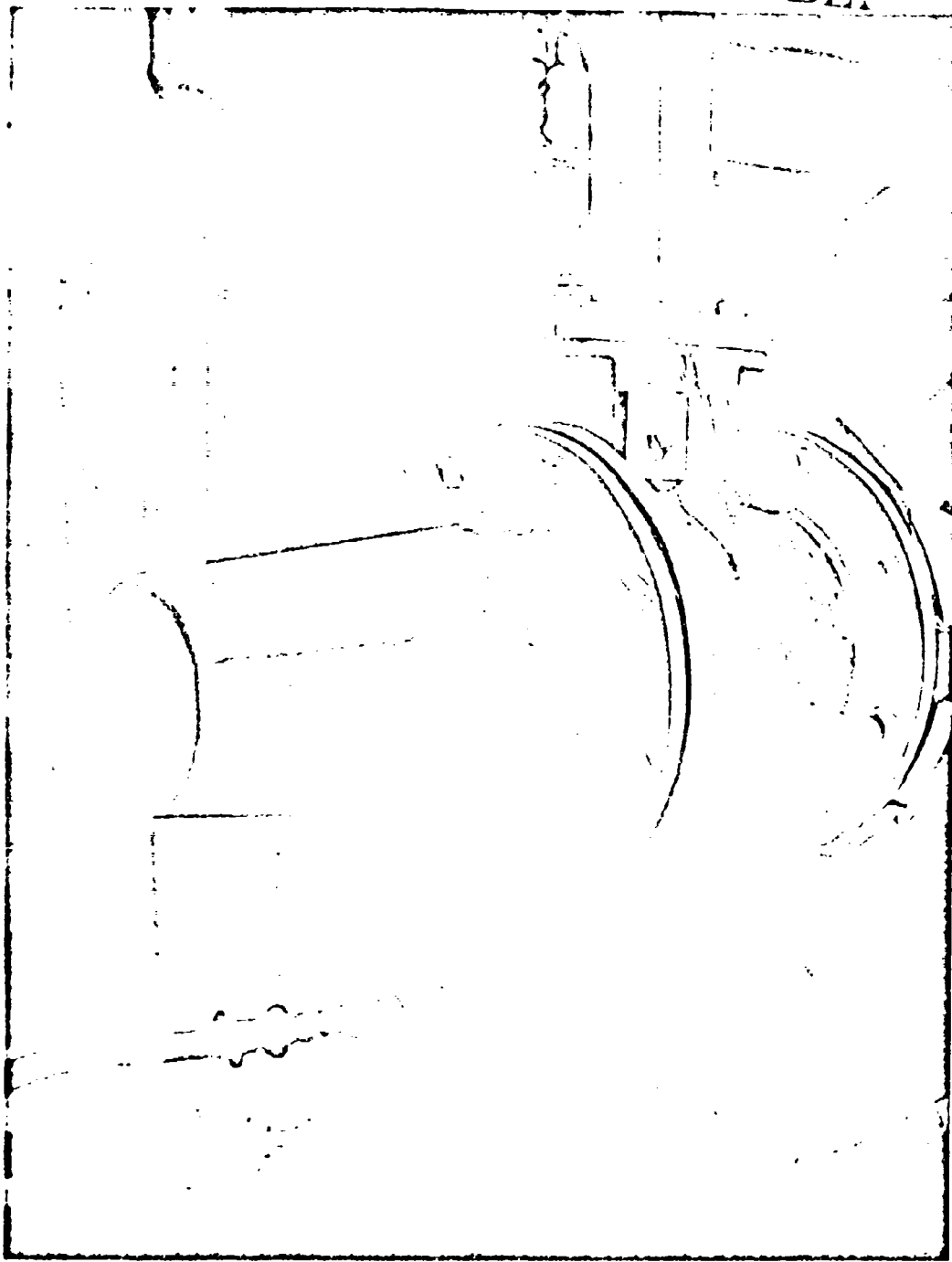


Figure 6. Nozzle and overpressure supply lines.

NOT REPRODUCIBLE



Figure 7. Combustion chamber pressure transducer location. A water-cooled adaptor is used.

NOT REPRODUCIBLE



Figure 8. Intake and exhaust systems pressure transducer locations. Water cooled adaptor is used for the exhaust system transducer.

LIMITED PRESSURE DIESEL CYCLE

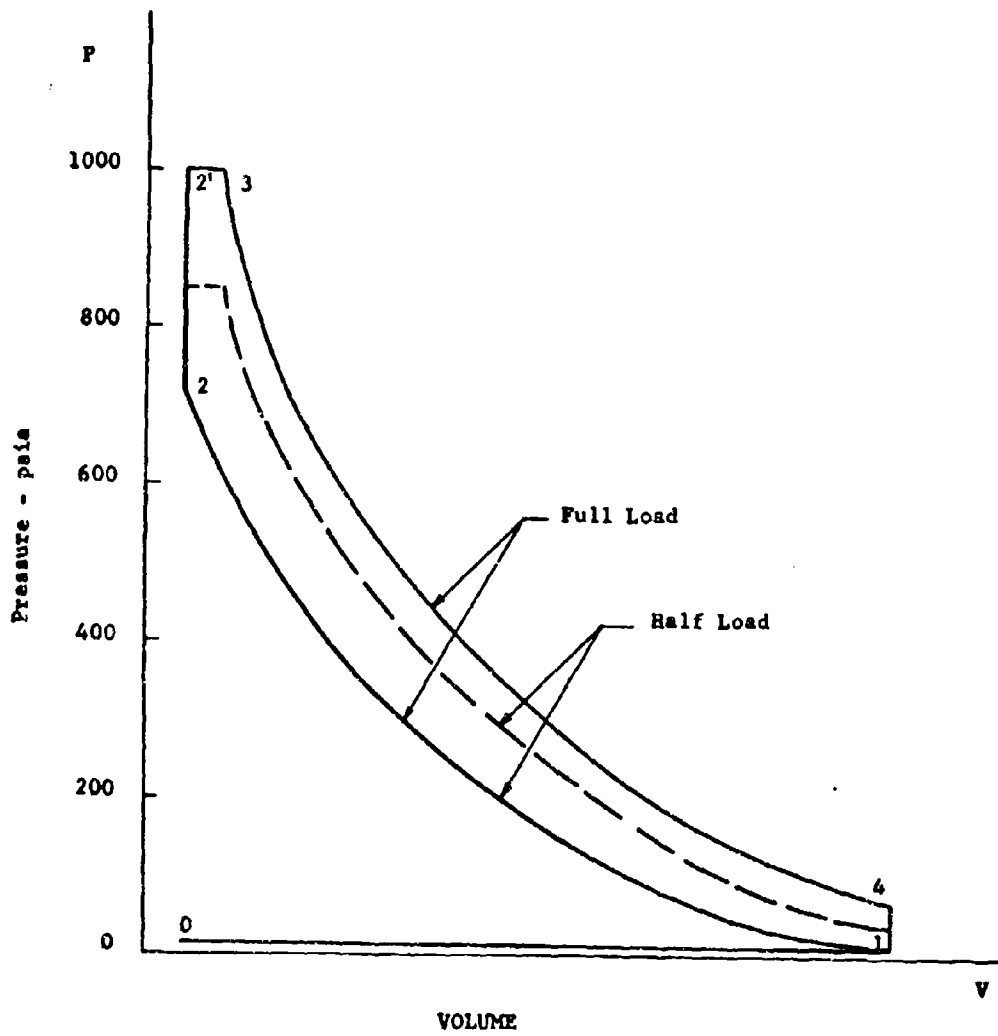


Figure 9. PV diagrams of full load and one-half load engine operation.

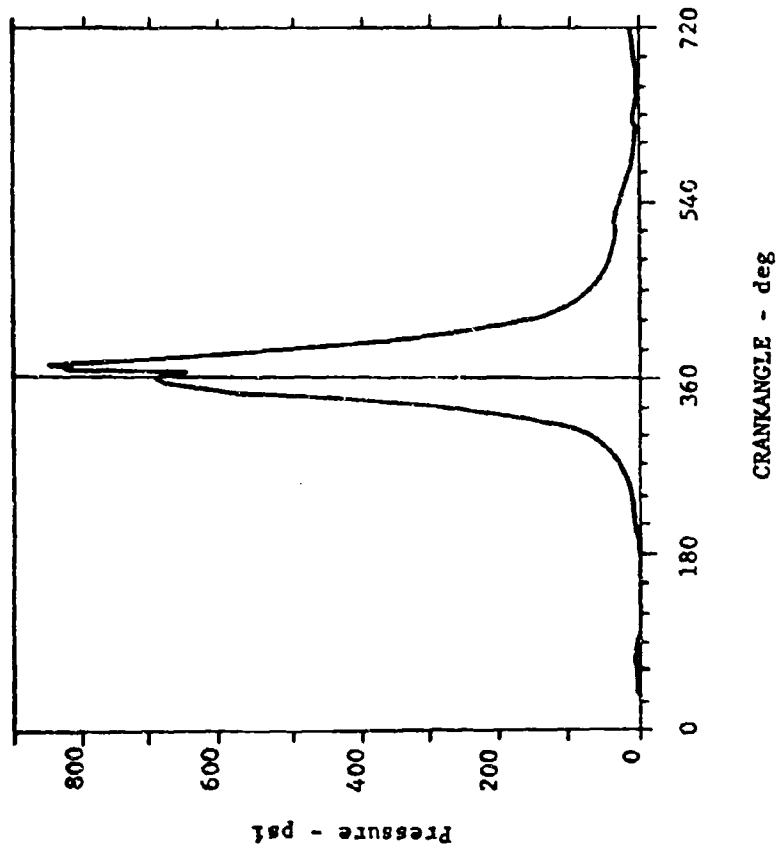


Figure 10. Precombustion chamber pressure-time diagram, Cylinder No. 4, Waukesha 180 DLC engine, 1800 rpm, one-half load.

ENGINE CYCLE EVENTS

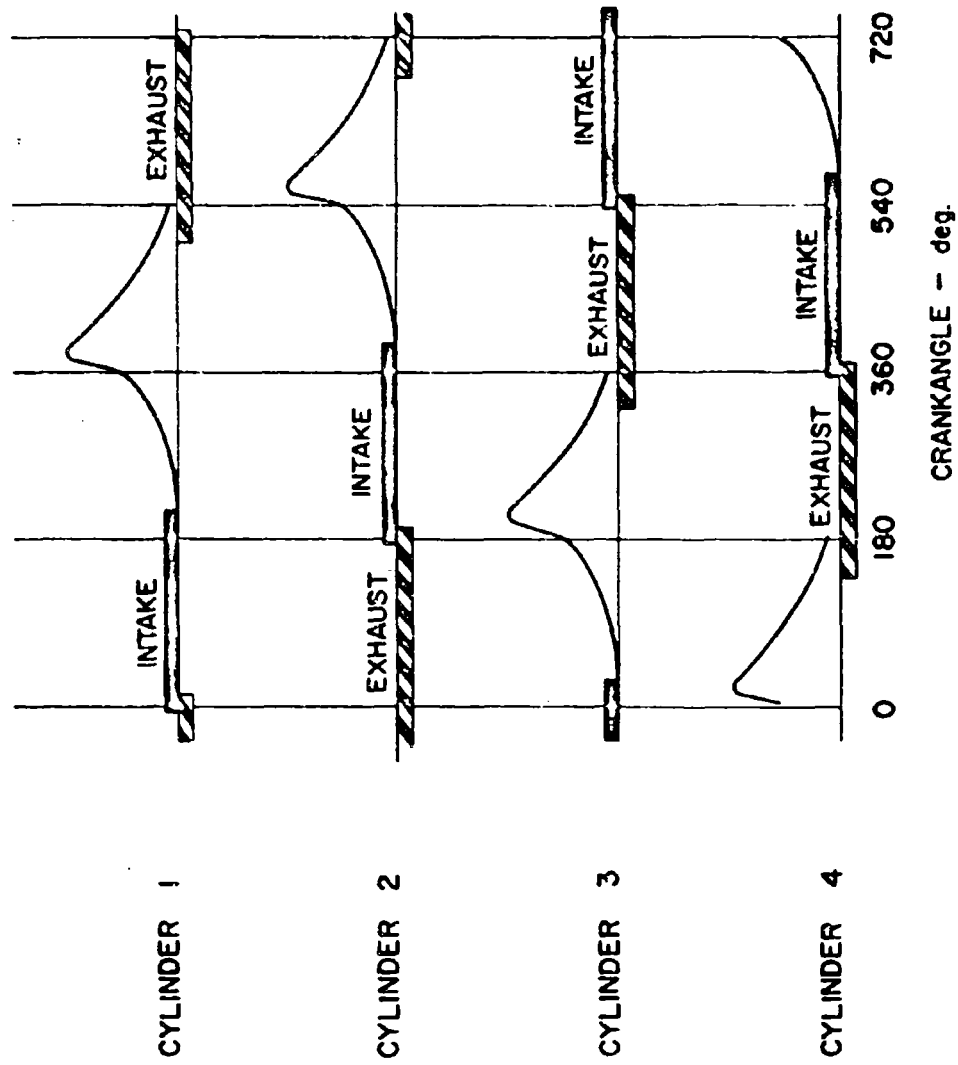


Figure 11. Engine cycle events for all four cylinders of the Waukesha engine showing one complete cycle.

PRESSURE TIME OSCILLOGRAMS

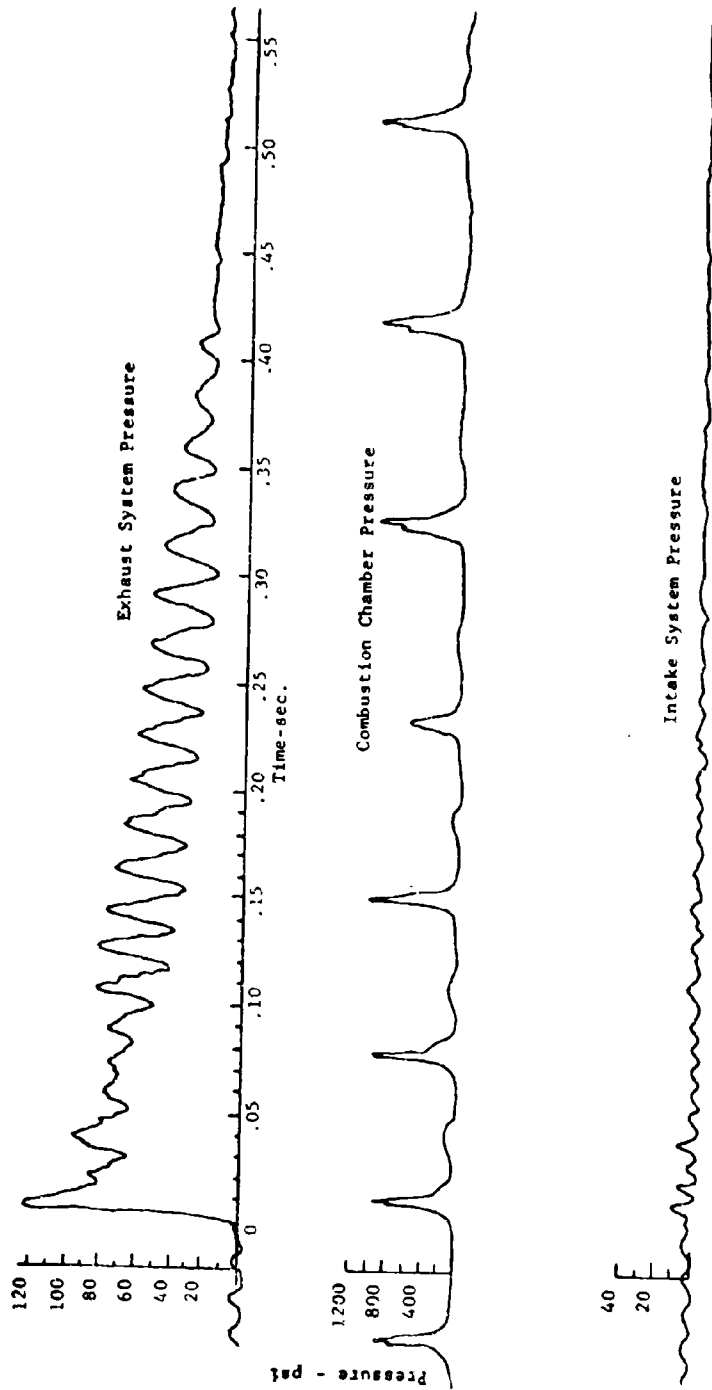


Figure 12. Pressure-time diagrams for 100 psi exhaust system overpressure application.

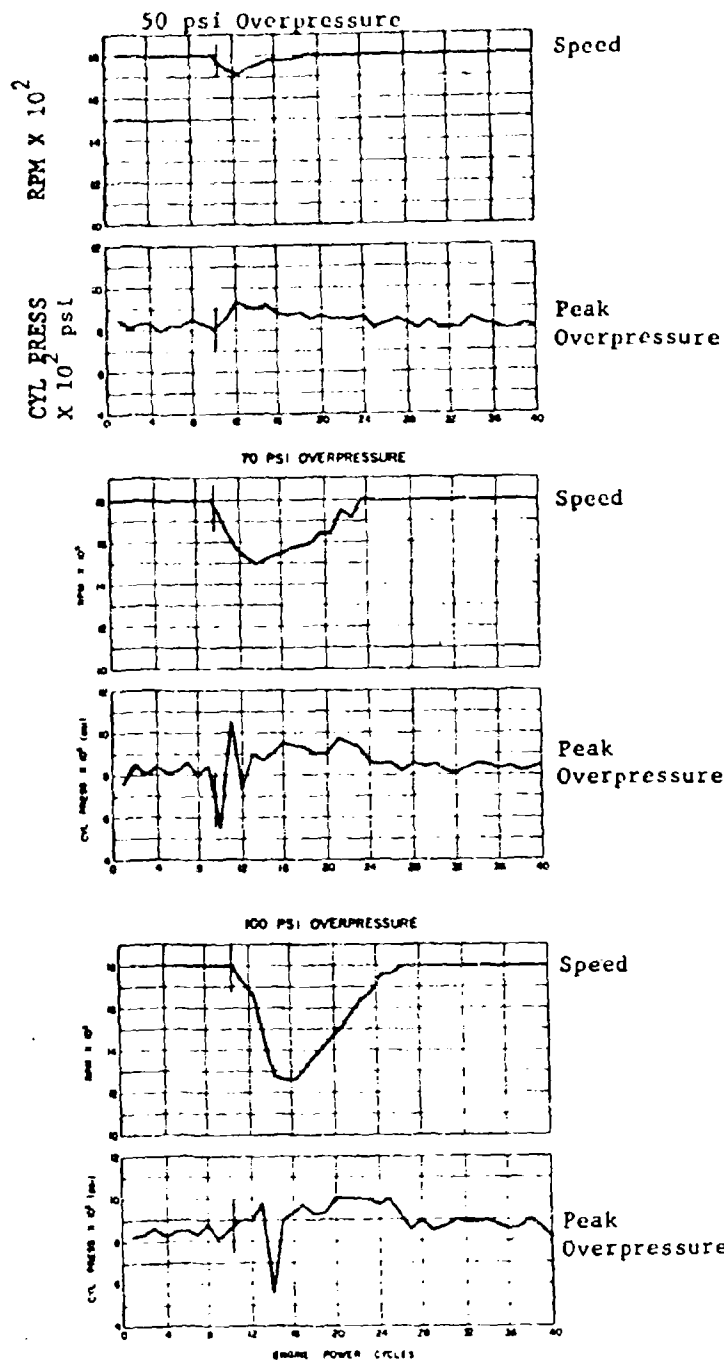


Figure 13. Speed and combustion chamber peak pressure variations with exhaust system overpressure applications. Overpressure application begins after engine cycle 10 indicated by a vertical line.

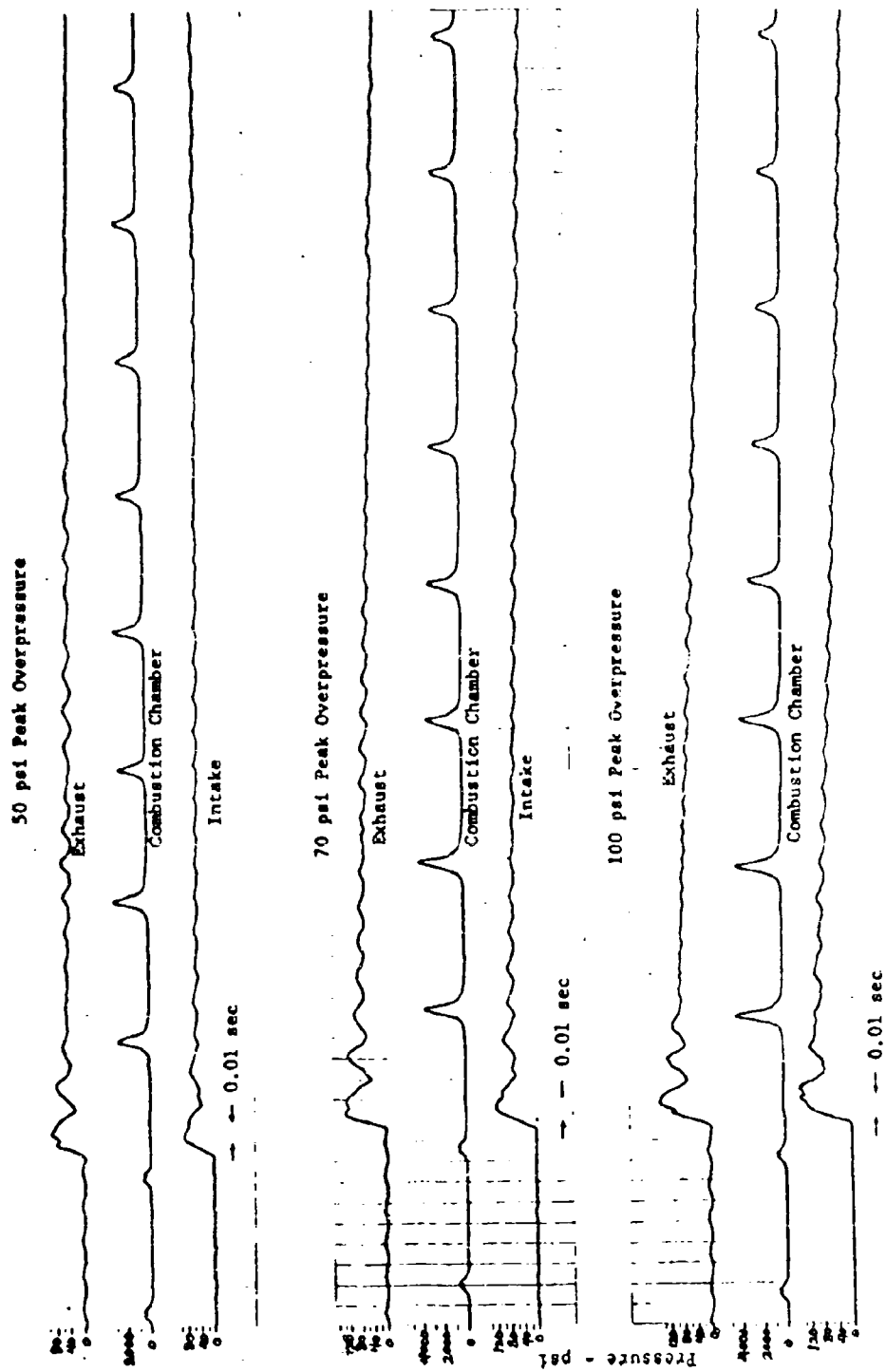


Figure 14. Intake and exhaust system overpressure application oscillograms.

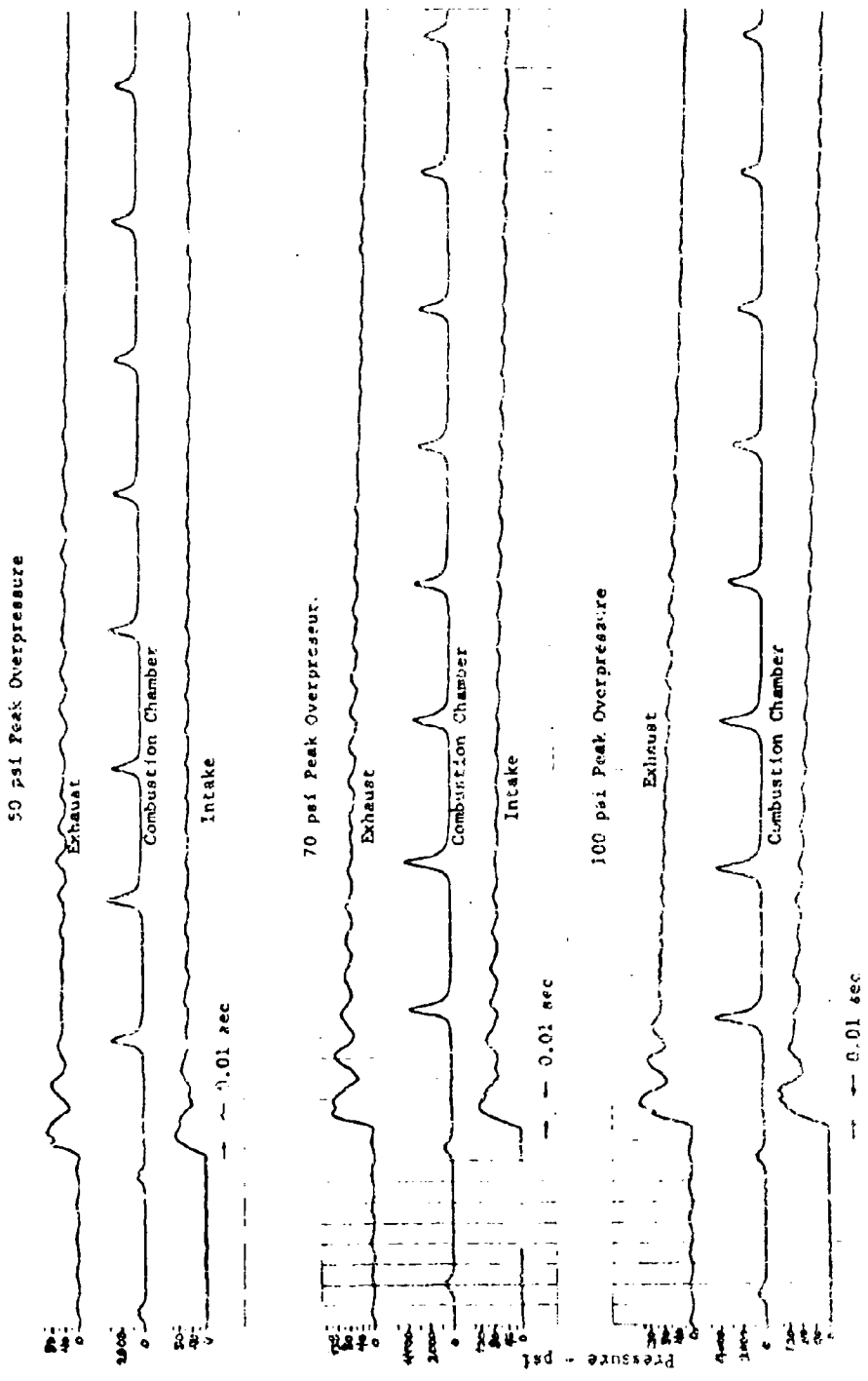


Figure 14. Intake and exhaust system overpressure application oscillograms.

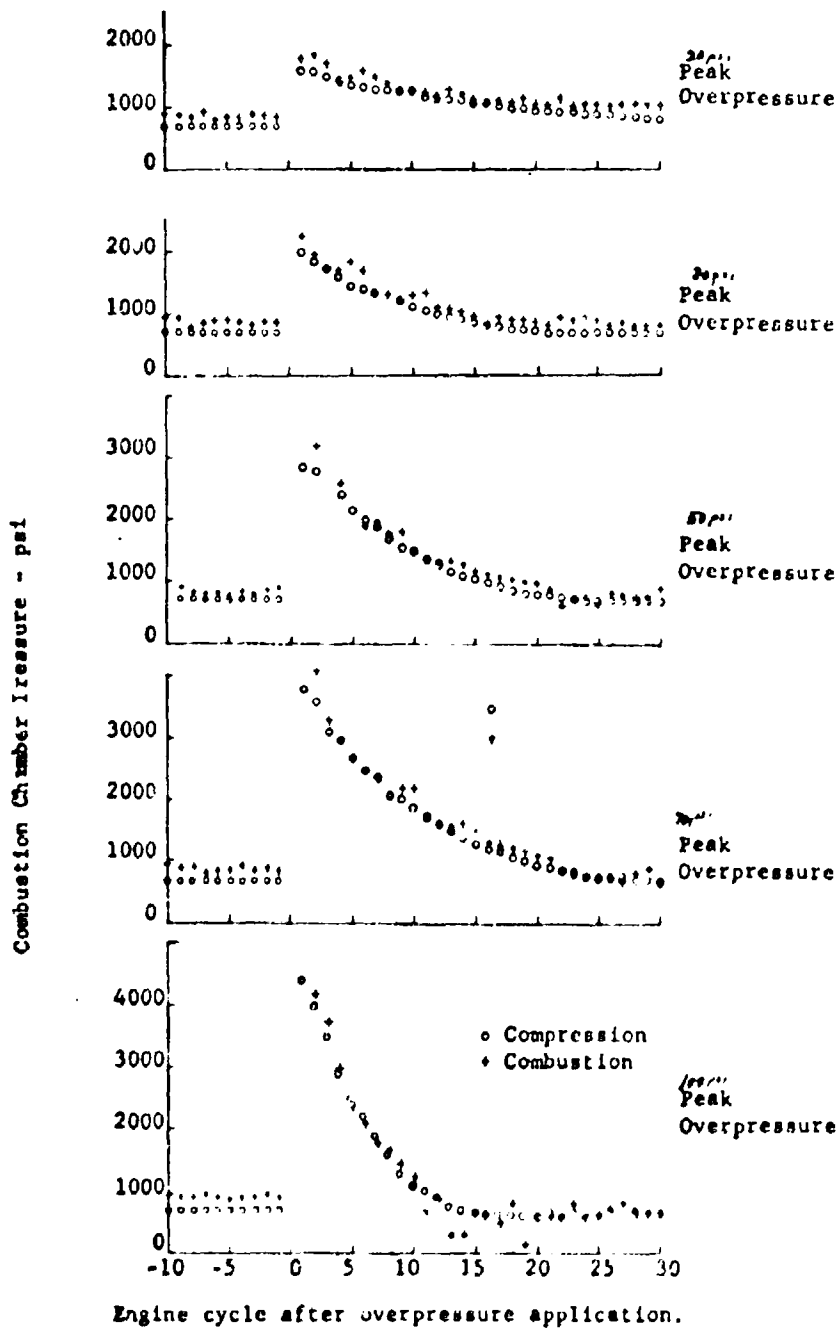


Figure 15. Compression and combustion peak pressures before and after overpressure applications.

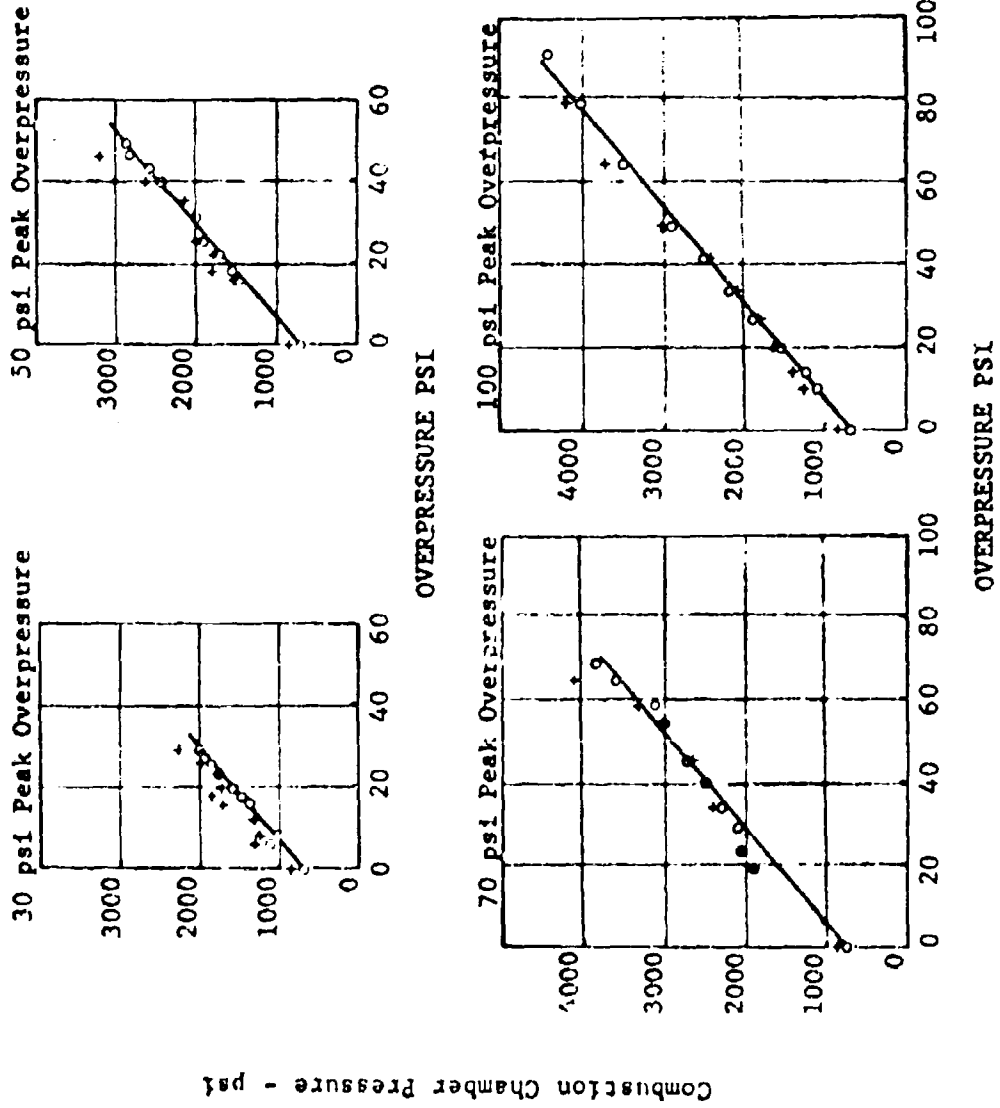


Figure 16. Peak combustion chamber pressures compared with overpressure exposure pressure.

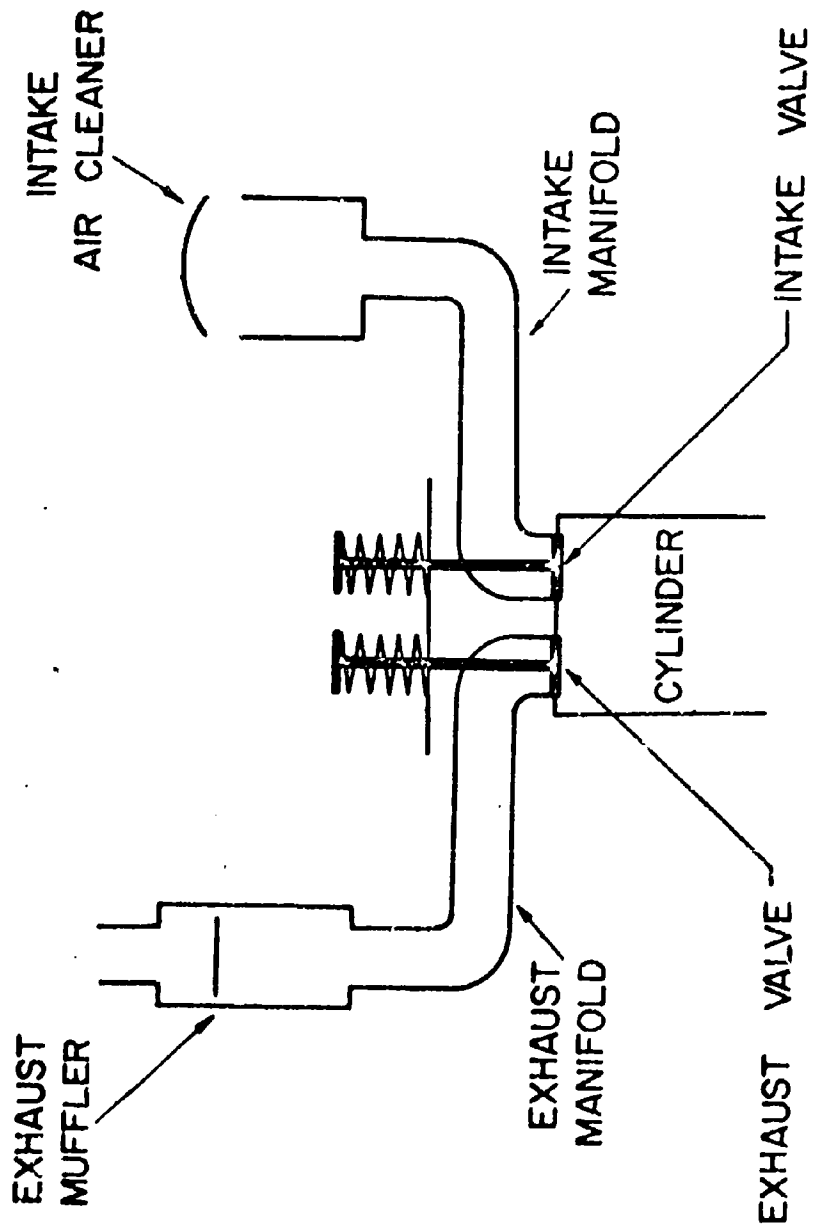


Figure B1. The engine's intake and exhaust systems.

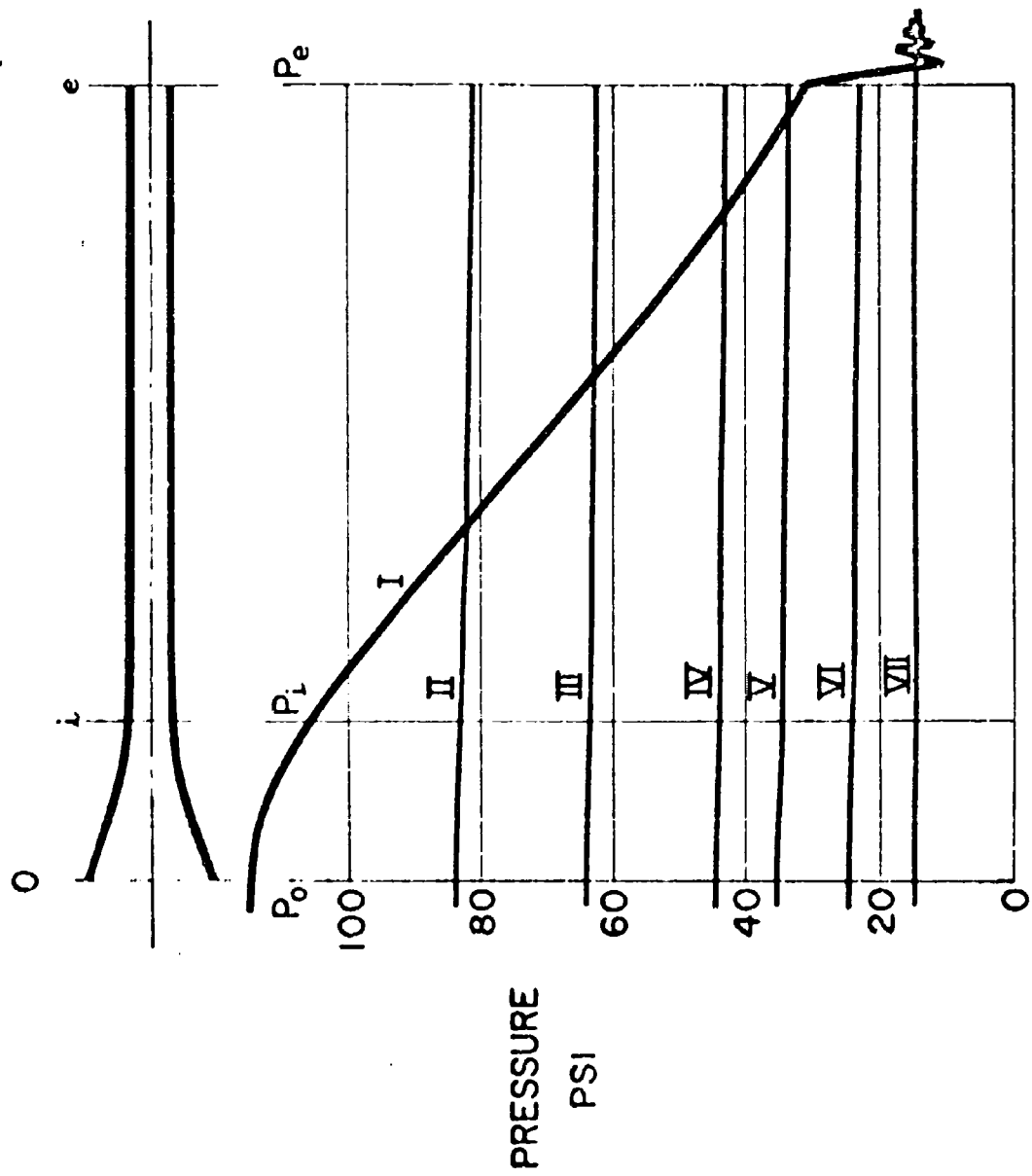


Figure B2. Pressure distribution in assumed engine intake or exhaust system.

70 PSI PEAK OVERTRESSURE

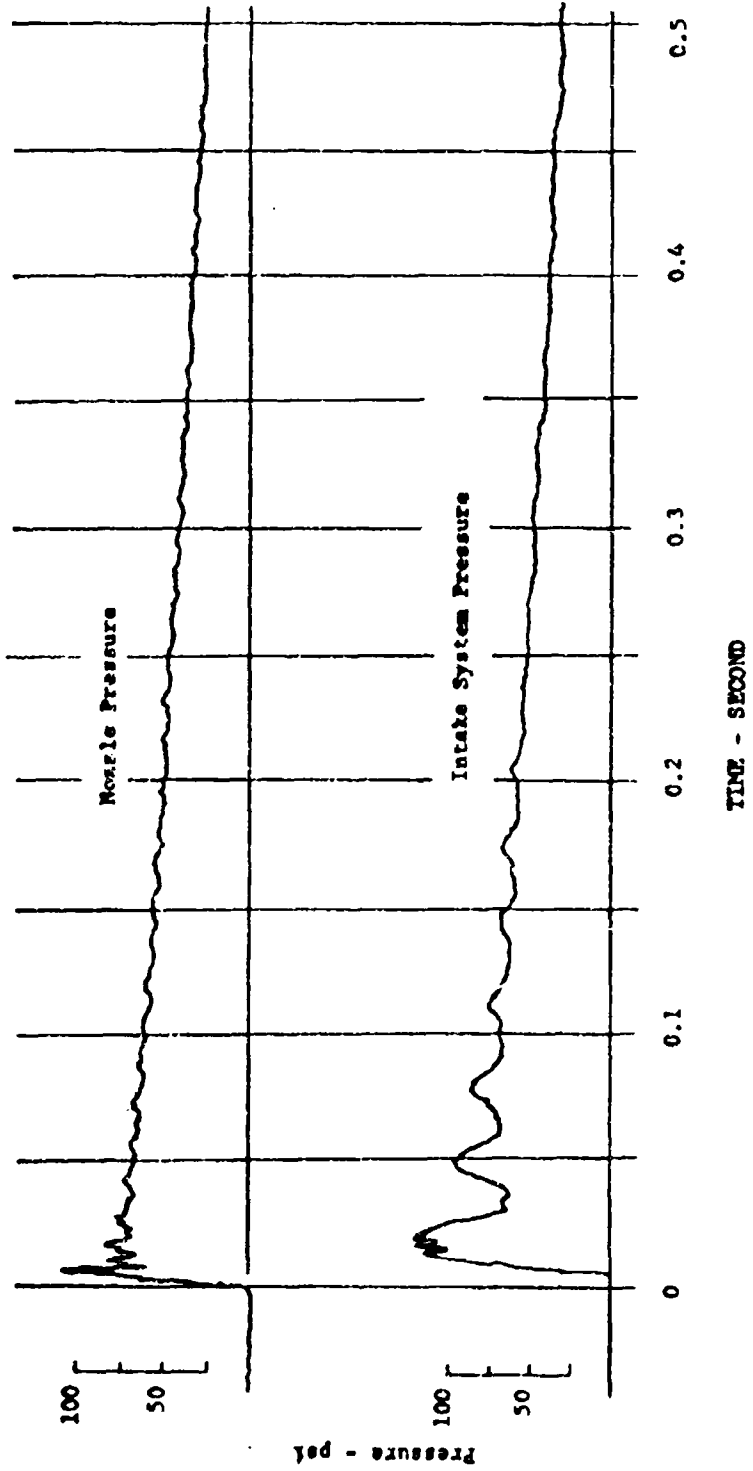


Figure B3. Intake system pressure-time record compared with nozzle entrance pressure-time record.